KeAi
CHINESE ROOTS
GLOBAL IMPACT

Contents lists available at ScienceDirect

Petroleum Science

journal homepage: www.keaipublishing.com/en/journals/petroleum-science



Original Paper

Evaluation of cement density utilizing through-casing X-Ray logging method



Ji-Lin Fan ^{a, b}, Qiong Zhang ^{a, *}, Ya Jin ^c, Quan-Wen Zhang ^c

- a School of Automation Engineering, University of Electronic Science and Technology of China, Chengdu, 611731, Sichuan, China
- ^b China National Logging Corporation, Xi'an, 710077, Shaanxi, China
- ^c China Oilfield Services Limited, Sanhe, 065201, Hebei, China

ARTICLE INFO

Article history: Received 23 June 2024 Received in revised form 5 September 2024 Accepted 7 November 2024 Available online 9 November 2024

Edited by Meng-Jiao Zhou and Min Li

Keywords: X-ray source Cement density Optimization technique

ABSTRACT

In the evaluation of cementing quality, quantitatively assessing cement density is crucial along with identifying the cementation degree at the interface using acoustic logging. While the ¹³⁷Cs-based formation density logging method is well-suited for density calculation, its reliance on open-hole environmental measurements poses challenges when inspecting cement density. This work focuses on the quantitative calculation of cement density while considering the radioactive hazards to the environment caused by ¹³⁷Cs source. The proposed approach utilizes a measurement system consisting of an X-Ray source and four gamma detectors. The gamma spectrum characteristics of each detector are analyzed, and the energy spectrum recorded by each detector is distinguished by different energy windows. A forward model is established to relate the gamma counts of each energy window to the formation and cement parameters. By employing a regularized Newton's method based on optimization technique, cement density can be calculated with a controllable error margin of within 0.015 g/cm³. Furthermore, even though X-Ray detection has lower sensitivity to formation parameters compared to ¹³⁷Cs, this method is capable of estimating formation density. Overall, the proposed approach enables the quantitative calculation of cement density and semi-quantitative calculation of formation density, therefore is of significance to the comprehensive evaluation of cementing quality.

© 2024 The Authors. Publishing services by Elsevier B.V. on behalf of KeAi Communications Co. Ltd. This is an open access article under the CC BY license (http://creativecommons.org/licenses/by/4.0/).

1. Introduction

The measurement of medium density using gamma ray is a well-established technique. Baker (1957), Wahl et al. (1964), and Bertozzi et al. (1981) investigated methods for density logging using ⁶⁰Co/¹³⁷Cs sources and gamma ray detectors, and the pioneering work illustrated the feasibility of utilizing gamma rays for measuring formation density. With the development of density logging technology, the introduction of the three-detector density logging tool by Eyl et al. (1994) significantly improved density detection accuracy and longitudinal resolution. Advancements in controllable sources led to the development of techniques for calculating formation density using secondary gamma rays generated by pulsed neutron sources or X-Ray sources. Wilson (1995) proposed the theory of pulse source neutron gamma density logging, while Odom et al. (1999) utilized pulsed neutron logging tool

* Corresponding author. E-mail address: zhanqio@uestc.edu.cn (Q. Zhang). to measure the ratio of inelastic and capture gamma counts for formation density characterization. Subsequent contributions by Reichel et al. (2012), Guo et al. (2014), Zhang et al. (2023), and others have further expanded on controllable neutron density logging methods, enhancing the capabilities and accuracy of density measurements in various geological settings.

Building upon X-Ray density logging technology, Becker et al. (1987) and Bayless et al. (1993) were pioneers in utilizing X-Ray accelerators to replace ¹³⁷Cs sources for density logging, laying the foundation through experimental research. However, challenges related to temperature constraints and the miniaturization of X-Ray generators, it was not until 2018 that Schlumberger introduced the first commercially available four-detector X-Ray density logging tool (Simon et al., 2018). Leveraging this detection system, Zhang et al. (2023) introduced a sophisticated multi-window and multi-parameter inversion algorithm capable of real-time calculation of various formation and mud cake parameters. Moreover, X-Ray technology has enabled physical imaging of rock samples on the ground. Wilson (1995) and Jussiani and Appoloni (2015) employing different energy X-Ray to reconstruct the atomic number of rock

samples to produce images depicting sample density. Recent studies by Wang and Zhang (2023) and Li et al. (2023) explored digital radiography (DR) utilizing X-Ray technology, demonstrating that flexible detectors like the CsPbBr₃ crystal detector exhibit exceptional performance in X-Ray imaging. These studies show-cased the potential for enhanced imaging and analysis in geoscience applications of X-Ray technology.

In the realm of evaluating cementing quality, the integration of density logging and acoustic logging has proven to be a valuable approach (Dowell et al., 1999; Thierry et al., 2016; Li et al., 2019). Specifically, in cased well, the utilization of multi-detector gamma spectrum data processing facilitates the extraction of crucial cement density information. Historically, Moake (1998) engineered a four-detector density logging tool for cased wells, which realized simultaneous measurement of casing thickness, cement density, cement thickness and formation density. Hu and Guo (2015) developed a method to assess cementation quality by analyzing the energy spectrum data recorded by density logging tool. Recent advancements have further enhanced the capabilities of cement evaluation techniques. Zhang (2024) introduced an innovative approach utilizing a three-detector density logging tool for detecting formation density and Pe despite mudcake presence, enabling independent determination of mudcake thickness and formation density. Li (2023) established a forward model based on a multi-detector density logging system, enabling the measurement of formation density through casing via multi-detector and multi-window gamma counts. While existing research primarily focuses on formation density calculations, efforts aimed at improving the accuracy of cement density calculations continue to be a priority, highlighting the ongoing quest for enhanced precision in cement evaluation methodologies.

This manuscript presents a four-detector density measurement system based on X-Ray and the interaction theory between gamma rays and medium. X-Ray energy is lower and its detection range is narrower than ¹³⁷Cs source, making it more sensitive to cement density. The corresponding relation set of X-ray photon counts from different detectors to cement and formation parameters are established, enabling the inverse calculation of cement density using optimization methods for high accuracy. This study aims to provide technical guidance for comprehensive evaluation of cementing quality and may offer reference for the development of subsequent through casing X-Ray logging tool.

2. Methodology

Unlike single-energy gamma ray emitted by the ¹³⁷Cs source, X-Ray emits lower energy photons with continuous energy distribution. The interaction between X-Ray and formation medium is primarily multiple attenuation and scattering of gamma ray. In the scenario of an intact casing, the cased well environment can be considered as a dual medium consisting of cement and formation. The attenuation of X-Ray in this context can be described as

$$I_1 = I_0 e^{-\mu \rho x} \tag{1}$$

where I_1 and I_0 are the transmitted and incident intensity, respectively, μ is the attenuation coefficient of the medium, ρ is the density of the medium, and x is the distance that the X-Ray travels through the medium.

If X-Ray is scattered in a medium, the following equation is satisfied:

$$I_{1}^{\prime}=I_{0}^{\prime}\frac{\mathrm{d}\sigma(E,\Omega)}{\mathrm{d}\Omega}S(E,\theta,Z)\mathrm{d}\Omega\rho N\frac{Z}{A}A_{s}\Delta L \tag{2}$$

where I_1' and I_0' are the gamma intensity before and after scattering, $d\sigma(E,\Omega)/d\Omega$ is the differential scatter cross-section, $S(E,\theta,Z)$ is the incoherent scattering function, E is the energy of photons before scattering, θ is the scatter angle, $d\Omega$ is the solid angle subtended by the detector, V is voxel volume, numerically equal to the product of source beam area A_S and voxel thickness ΔL . ρ is the density at scattering point.

Therefore, after multiple attenuation and scattering of X-Ray in the dual medium under the cased well environment, the gamma flux received by the detector can be expressed as

$$I = I_0 \prod_{i=1}^{m} (e^{-\mu \rho x})_i \prod_{i=1}^{n} \left(\frac{d\sigma(E, \Omega)}{d\Omega} S(E, \theta, Z) d\Omega \rho N \frac{Z}{A} V \right)_j$$
 (3)

where I is the detected gamma intensity, and I_0 is the X-Ray source intensity. i and j are the numbers of attenuation and scattering in the interaction of X-Ray and dual medium, respectively.

Therefore, from Eq. (3), we can see that X-Ray detection is determined by the density of the dual medium, the attenuation coefficient of the medium, X-Ray energy and the parameters related to scattering. For a certain detector of the logging tool, its spacing determines that its detection depth is fixed, cement thickness is therefore also a key parameter in determining the density of the medium within the detection range. Therefore, gamma ray detection is affected by four parameters: cement density (ρ_c), cement thickness (h_c), formation density (ρ_b), and formation volume photoelectric absorption cross section index (U_b), which can be expressed as

$$I = f(\rho_{c}, h_{c}, \rho_{b}, U_{b}) \tag{4}$$

After determining the key parameters influencing gamma ray detection, it is vital to establish a comprehensive forward model to underpin subsequent cement density inversion. Due to the lowenergy characteristic of X-Ray, gamma counts of each energy window are susceptible to the combined effects of formation lithology and density. To enhance the accuracy of the forward model, we introduced the cross-terms of density and volume photoelectric absorption cross section index into the forward model of gamma counts to formation parameters. Additionally, in conventional density logging, the relationship between gamma counts and density typically follows a linear pattern. By incorporating second-order terms of parameters into the forward model, we ensure the accuracy of fitting the coefficients in the forward model with a large amount of simulation data. Therefore, the final forward model expression is represented as

$$\begin{cases} N_{1}(\rho_{c}) = a_{1} + a_{2}\rho_{c} + a_{3}\rho_{c}^{2} \\ N_{2}(h_{c}) = b_{1} + b_{2}h_{c} + b_{3}h_{c}^{2} \\ N_{3}(\rho_{b}, U_{b}) = c_{1} + c_{2}\rho_{b} + c_{3}U_{b} + c_{4}\rho_{b}^{2} + c_{5}U_{b}^{2} + c_{6}\rho_{b}U_{b} \end{cases}$$
 (5)

where, N is the gamma counts under different energy windows, and the three equations respectively represent the forward response relationship of gamma counts with cement and formation parameters. a, b, and c are the constant coefficients, which are obtained from data fitting via a significant amount of numerical simulations.

Then, how to achieve the inverse calculation of cement density is more important. Once the influence of the above four parameters on the gamma counts of different energy windows of each detector are investigated, it will be possible to find the optimal solution of cement density or even formation density by multi-parameter inversion through the idea of optimization.

Based on the forward model established above, the regularized Newton's method is used to solve the formation and cement parameters. As multiple parameters change, the energy spectrum information received by the detector will change accordingly. In each energy window interval, gamma flux will generate different results from the given standard condition ($N_{\rm st}$). It is possible to consider the variation in count difference within each energy window because of combined influences from formation and cement parameters. This variation can be effectively described as a linear combination of counting rate differences caused by these factors, then for each energy window:

$$\Delta N_i = \sum_{i=1}^3 (f(p) - N_{\rm st})_i \tag{6}$$

where f(p) represents the forward model of gamma counts in each energy window to the formation or cement parameter, and i is the number of formation and cement parameters. Therefore, the problem can be reformulated as an optimization problem:

$$F(x) = \Delta N_i - \sum_{i=1}^{3} (f(p) - N_{st})_i = 0$$
 (7)

Here, x represents all parameters to be inversed. The objective function F(x) in Newton's method is iteratively optimized using the equation:

$$x^{k+1} = x^k - \alpha_k H(x^k)^{-1} \nabla F(x^k)$$
(8)

where α_k represents step factor, H(x) is second order partial derivative matrix of F(x). The optimal solution to the problem can be obtained by multiple iterations.

To ensure accuracy and stability in the iterative process of Newton's method, we employ the Tikhonov regularization method to reconstruct H(x) in this study. By controlling the number of singular values, we strike a balance between solution accuracy and iterative stability, ultimately leading to an accurate determination of cement density. The optimal solution to the problem is obtained by multiple iterations, the iteration is stopped when the difference in cement density between the two iterations is less than 0.015 g/cm³.

3. Response model development

FLUKA (Battistoni et al., 2007) is a general-purpose Monte Carlo particle transport tool that runs on Linux and UNIX systems, which can be used for neutron, photon, electron or coupled neutron/photon/electron transport, with wide application in such scientific fields as particle transport, radiation protection and radiometry, radiation shielding design optimization, and detector design and analysis. In this study, FLUKA is utilized to establish logging tool and formation models for analyzing gamma spectrum characteristics under varied cement and formation parameters. The aim is to develop a relationship set between gamma counts of different energy windows with cement and formation parameters, laying the precondition for optimal cement density inversion.

3.1. The model of formation and X-Ray logging tool

In reference to the structure parameters of the X-ray density logging tool introduced by Schlumberger, a four-detector and an X-Ray source logging tool is established, as illustrated in Fig. 1. Under the formation condition of 140 cm in both height and diameter, the

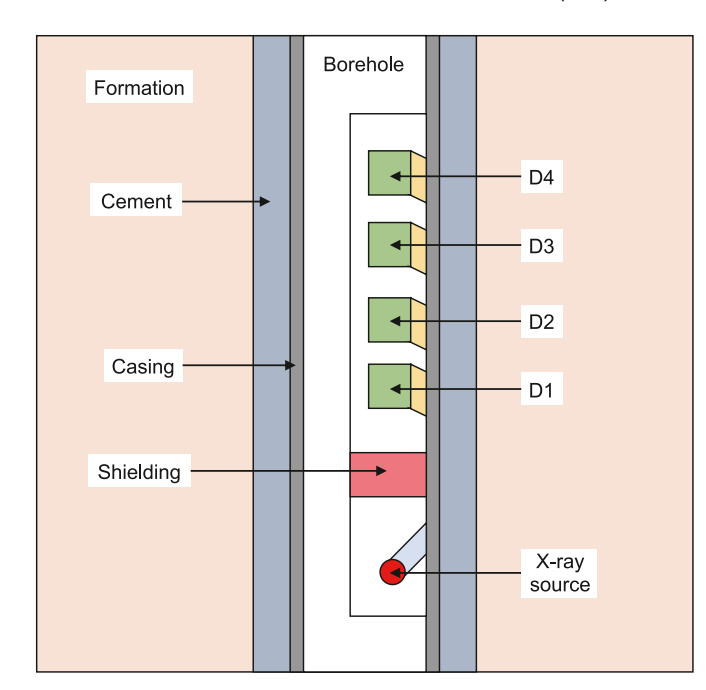


Fig. 1. Numerical simulation model of formation and X-ray logging tool.

borehole is 20 cm diameter size and filled with fresh water. Sandstone, limestone and dolomites as a formation matrix, the formation porosity changes from 0% to 40%, with freshwater used as pore fluid. The mixture of CaSiO₃ and water is used as cement with different thickness. The casing is made by steel and its thickness is 0.7 cm. The logging tool adopts the distribution type of X-Ray with the peak value of 0.15 MeV as the controllable source, to emit photons of 0.1–0.35 MeV energy to the formation. Tool housing is 0.5 cm thick, made with 17-4 PH steel. The X-Ray source and the detectors are separated by the shields. Gadolinium silicon oxide (GSO) is selected as the detector crystal for the four detectors, and an opening is designed to receive more scattered photons from formation. The source distances are 6, 12, 18 and 23.5 cm, respectively. The crystal size of the four detectors is identical: the diameter is 3.6 cm and the length is 4 cm.

3.2. Comparison of energy spectrum characteristics

Based on the established model, it is essential to investigate the impact of both cement and formation parameters on the gamma spectrum characteristics recorded by each detector. To achieve this, we initially established a standard condition, under which we varied the cement and formation parameters. Subsequently, we simulated the energy spectrum of the four detectors and analyzed the energy spectrum characteristics. The set standard conditions include the following: the formation matrix is sandstone with a porosity of 20%, a density of 2.32 g/cm³, and cement density of 1.8 g/cm³, thickness of 3 cm. Four parameters are adjusted: cement density (ρ_c), cement thickness (h_c), formation density (ρ_f), and formation volume photoelectric absorption cross section index (U_f).

To study the influence of different cement and formation parameters on energy spectrum measurement, we utilized the control variable method to modify each parameter. This can be categorized into the following four types.

- 1) Adjusting the density of the cement from 2.2 to 1.2 g/cm³;
- 2) Modifying the thickness of the cement from 4 to 2 cm;

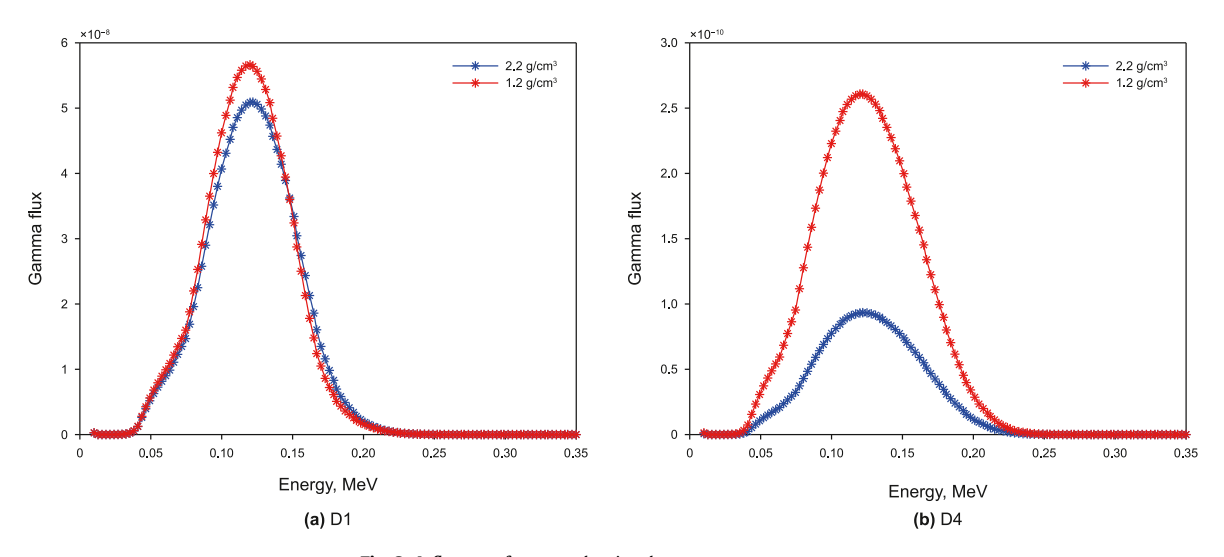


Fig. 2. Influence of cement density change on energy spectrum.

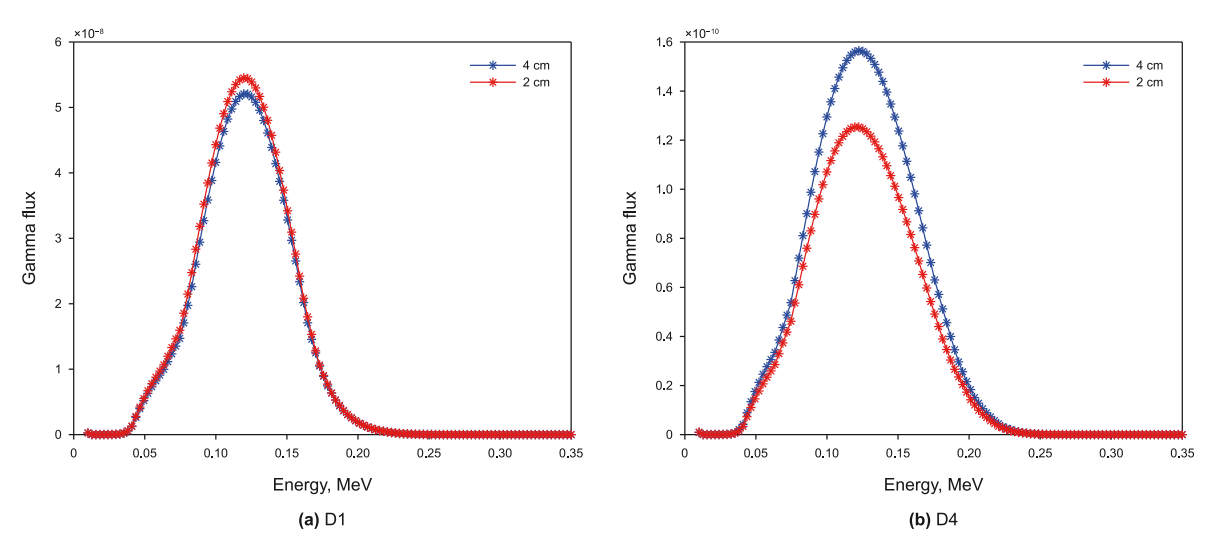


Fig. 3. Influence of cement thickness change on energy spectrum.

- 3) Controlling the formation matrix as sandstone, altering the porosity, and adjusting the formation density from 2.65 to 1.99 g/cm³;
- 4) Setting the formation medium as water-bearing sandstone and limestone, changing the porosity of both to control the density of the two to 3.32 g/cm³.

In these four numerical simulation experiments, the energy spectrum characteristics and the similarities and differences of the four detectors were analyzed, as depicted in Figs. 2–5. Due to the correlation between variations in the energy spectrum and spacing, only the energy spectra for detectors D1 and D4 are presented in the figure.

By analyzing the influence of cement parameters on gamma spectrum, it is evident that cement density plays a crucial role in gamma counts due to its proximity to the logging system outside the casing. In dual-media condition involving cement and formation, an increase in cement thickness leads to higher cement contributions within the detection range. Thus, lower density of cement results in an overall decrease in the average medium density within the detection range. The observed trend of

increasing gamma counts with decreased cement density or increased cement thickness aligns with density logging principles. However, Fig. 2 indicates a contrary pattern for the nearest detector D1 at spectral energies exceeding 0.15 MeV, which is also reflected in Fig. 3 across the full energy spectrum segment. This anomaly can be attributed to the presence of a high proportion of backscattered gamma ray in the recorded gamma ray, particularly when the spacing is in proximity. The backscattering of gamma ray tends to increase with an increase in medium density. Consequently, the attenuation and backscattering of gamma ray compete, causing the gamma spectrum obtained from the nearest spacing to display distinct distribution characteristics compared to those recorded by other detectors.

The variation of energy spectrum caused by the change of formation density is in line with changes in cement parameters. It should be emphasized that even under the same formation density, different lithologies can result in vastly different gamma counts recorded by the detector. Consequently, the impact of formation volume photoelectric absorption cross section index must be considered when calculating cement density, given that it plays a crucial role in gamma counts.

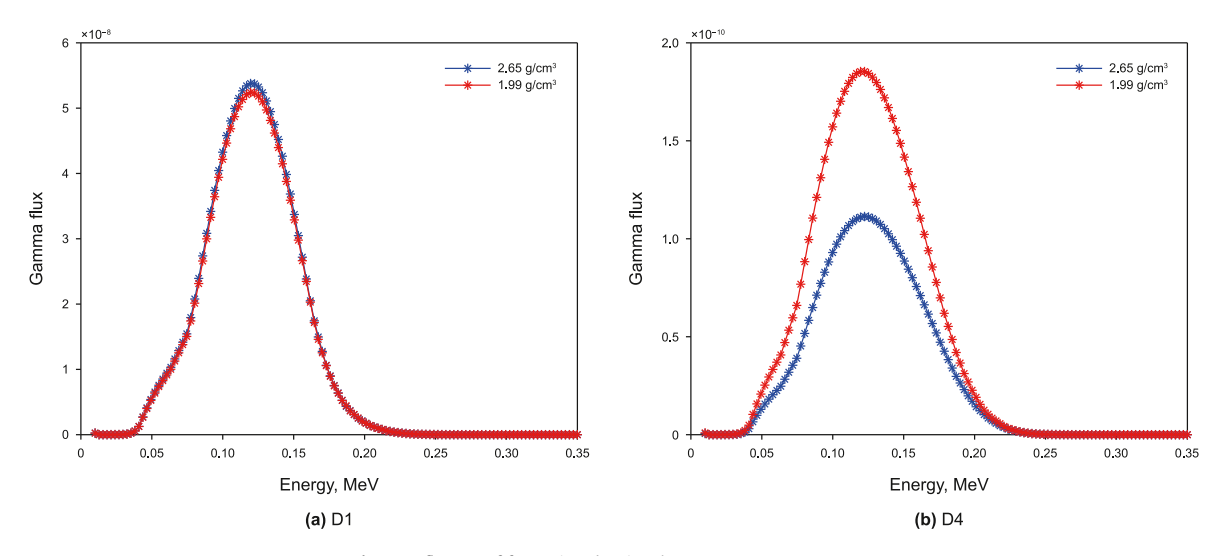


Fig. 4. Influence of formation density change on energy spectrum.

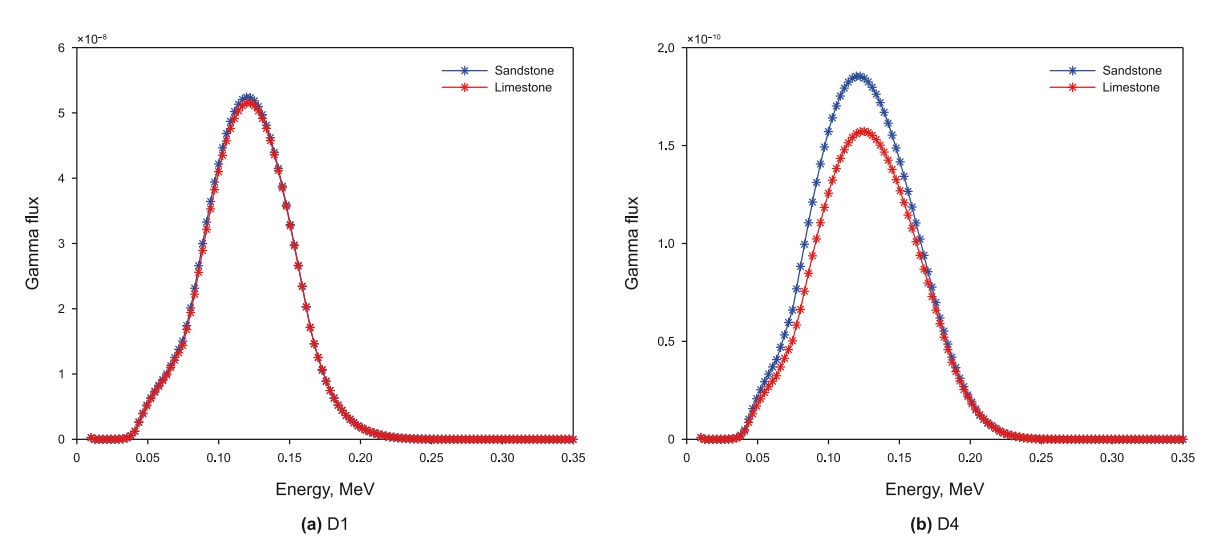


Fig. 5. Influence of formation volume photoelectric absorption cross section index change on energy spectrum.

3.3. Response model of gamma flux to cement and formation parameters

After studying the effects of formation and cement parameters on gamma spectrum characteristics, a substantial number of numerical calculation models needs to be established to fit the coefficients in the forward model and clarify the mathematical form of the forward model. This is the basis for subsequent cement density inversion work. Based on the standard conditions defined above, to ensure the accuracy of the inversion results, the energy spectrum measured by each detector is divided into multiple energy windows. By fitting the relationship between gamma counts and various formation and cement parameters within different energy windows, the response characteristics can be accurately determined. Fig. 6 shows the energy spectrum of the four detectors under the standard conditions.

The energy spectrum of different detectors exhibits similar distribution characteristics, allowing for the division of the energy spectrum into dual windows (0.08–0.11 MeV and 0.13–0.20 MeV) based on photoelectric effect and Compton scattering for the purpose of inversion calculation. Table 1 presents the gamma flux

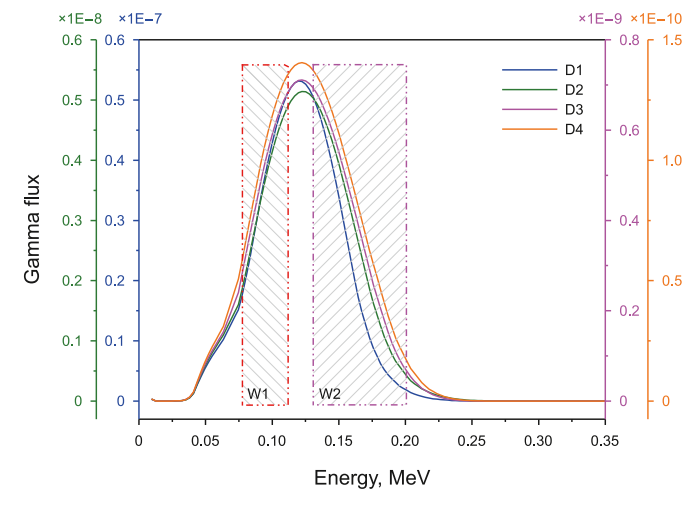


Fig. 6. The energy spectrum of the four detectors.

Table 1The gamma flux of four detectors under the standard condition.

Detector	D1		D2		D3		D4	
Energy window Energy window, MeV	W1 0.08-0.11	W2 0.13-0.2	W3 0.08-0.11	W4 0.13-0.2	W5 0.08-0.11	W6 0.13-0.2	W7 0.08-0.11	W8 0.13-0.2
Gamma flux,1E-9	417.731	520.168	40.755	65.001	5.919	9.333	1.204	1.942

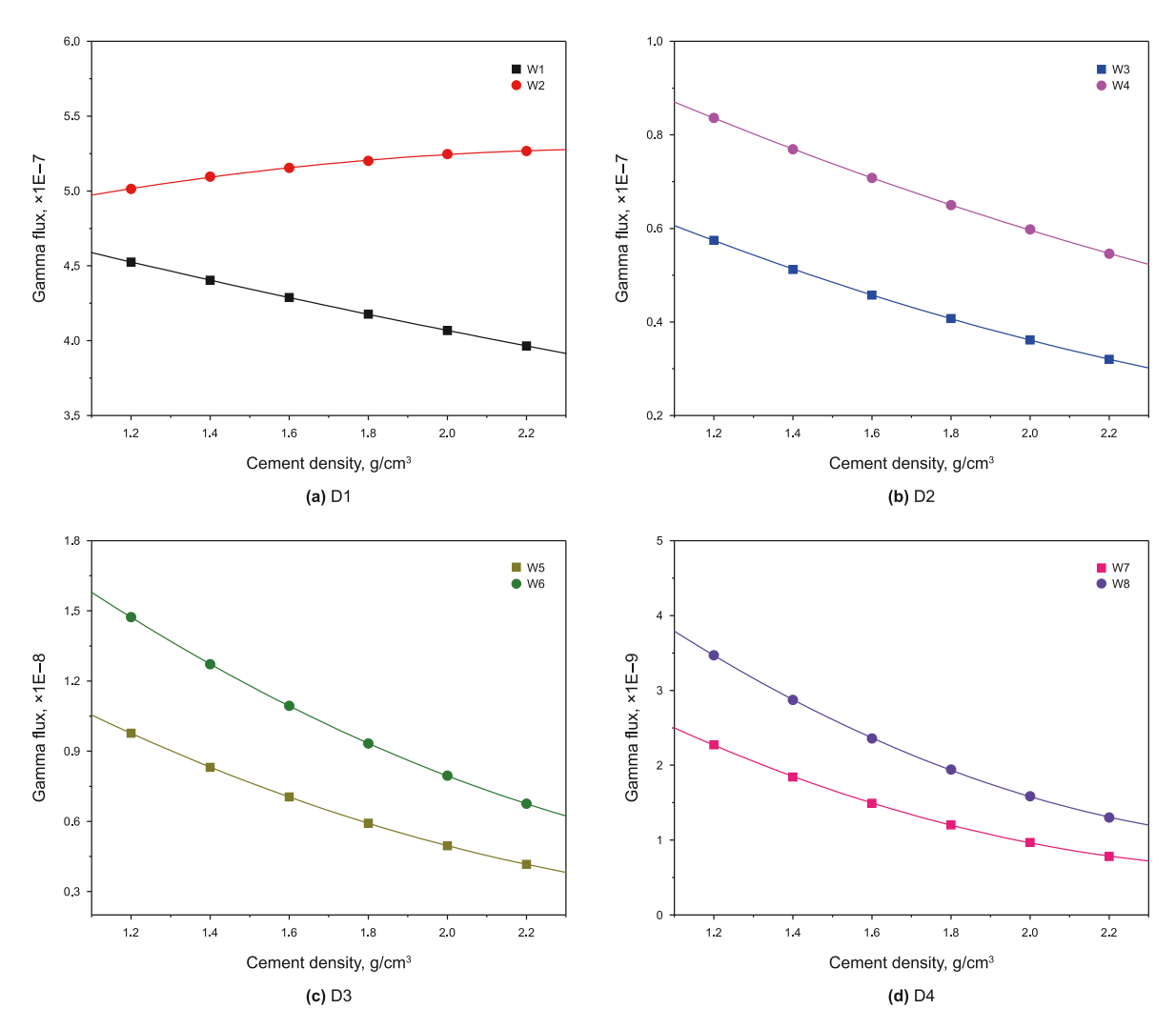


Fig. 7. The response of the gamma flux to cement density.

values recorded by the four detectors under standard conditions.

Then, Monte Carlo simulations are conducted to investigate the corresponding laws of gamma counts of different energy window with formation and cement parameters to obtain the response dataset for the subsequent cement density inversion work. For any combination of formation and cement parameters, the gamma flux of each energy window can be expressed as a function of the multiple parameters. The formation lithology is set as sandstone, limestone, and dolomite, with porosity ranging from 0% to 40%. The cement is varied in densities of 2.2, 2.0, 1.8, 1.6, 1.4, and 1.2 g/cm³. The thickness of the cement ranges from 2 to 4 cm, with intervals of 0.5 cm.

The model parameters are calculated using FLUKA to simulate the energy spectrum in various formation and cement conditions. Figs. 7 and 8 depict the response of the gamma flux to cement density and thickness, while Fig. 9 illustrates the response of the gamma flux to the formation parameters.

4. Result and discussion

To evaluate the effectiveness of the inversion algorithm, this study established several reservoirs and inverted multiple parameter values for verification. The formation matrix comprises sandstone, limestone, dolomite, and mixed lithology. Subsequently, the energy spectrum of the four detectors was simulated, and the gamma flux for the specified energy windows was calculated. Formation and cement information were then obtained through the inversion algorithm. Table 2 presents and the comparison between the actual values and the inversion values.

It is evident from the table that the obtained values for the inversion of cement density, cement thickness, and formation density closely align with the actual values. The calculation errors for cement density, of primary interest to us, consistently remain below 0.015 g/cm³ across the six model groups, exhibiting a level of accuracy comparable to that of open hole density measurements.

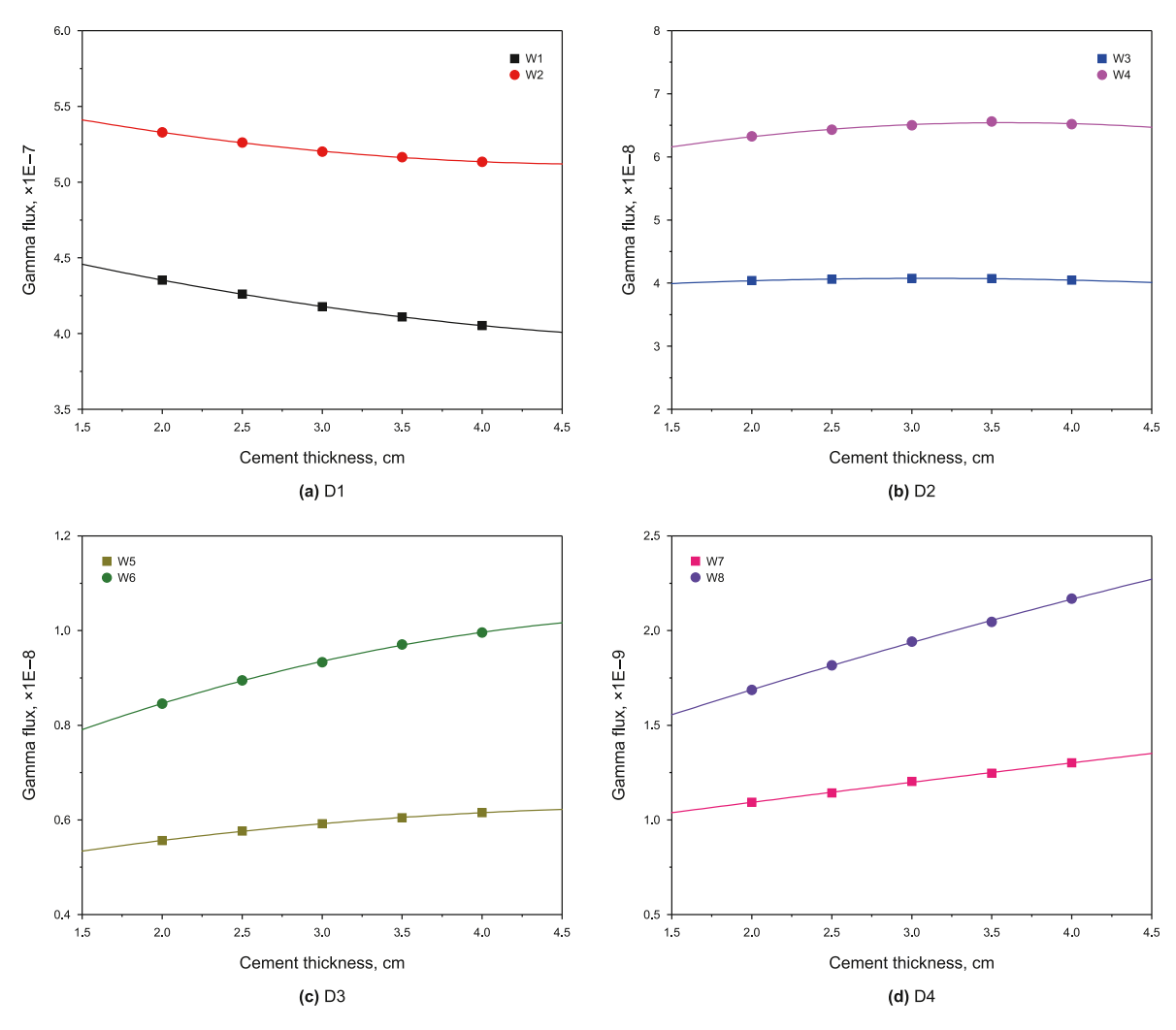


Fig. 8. The response of the gamma flux to cement thickness.

Furthermore, although the distance between the formation medium and the logging tool leads to lower accuracy than the cement density calculation, the formation density can still be reflected semi-quantitatively.

The following simulated example verifies the effectiveness of the proposed method to evaluate cement density. A cased well model is established. The casing thickness is 0.7 cm, and the formation is divided into 7 layers, each of which separated by shale, totaling 43 m. The parameters of each layer are shown in Table 3.

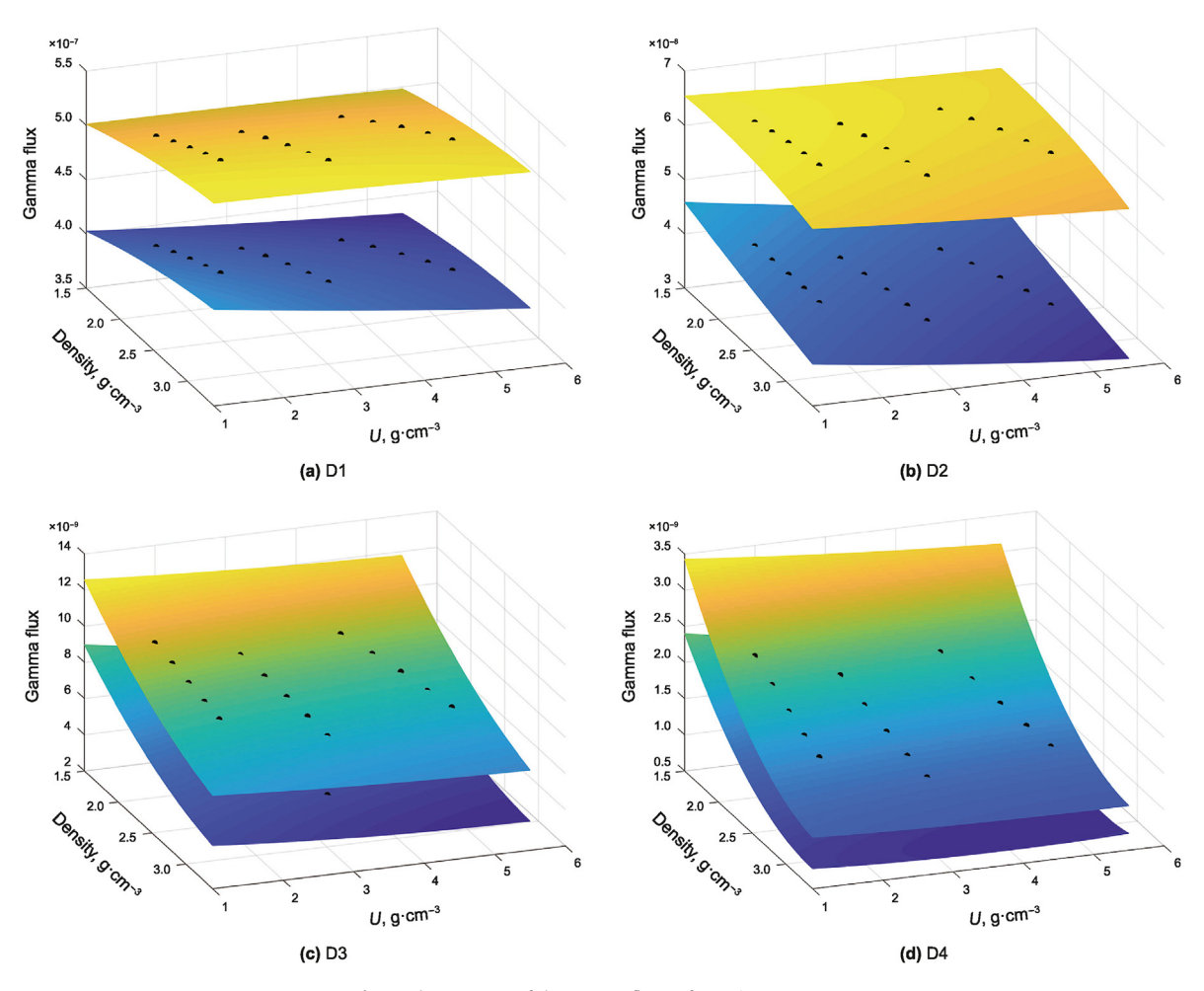
The gamma spectra from seven different layers are simulated using numerical simulation method, and then converted into gamma flux for the given energy windows. An interpolation algorithm is utilized to increase the number of measured data points, reflecting the movement of the logging tool slides against the well wall from top to bottom. Through the inversion algorithm, the cement and formation information are given in real-time. The final results are shown in Fig. 10. In addition to the depth track, the original lithologic section information is displayed in track 2. Tracks 3 to 8 show the comparison between the simulated and inverted values of cement and formation parameters, where the absolute error between actual values and inverted values of cement and formation parameters is marked respectively. Table 4 presents the inversion errors for formation density, cement density, and thickness.

Based on the results displayed in Fig. 10 and Table 4, the

inversion algorithm proves to be highly accurate across a range of reservoir conditions, including variations in lithology, porosity, cement density, and thickness. The algorithm consistently demonstrates minimal errors, with the absolute error in calculating cement density being kept within 0.015 $\rm g/cm^3$, showcasing its efficacy. Additionally, the algorithm controls the absolute errors in cement thickness and formation density within 0.3 cm and 0.04 $\rm g/cm^3$ respectively. Although the calculation accuracy of formation density and cement thickness is not as high as that of cement density, the algorithm still provides valuable information about cement thickness and formation density for reference.

5. Conclusion

In this study, a method to obtain cement density through casing using a four-detector X-Ray logging system is proposed, aiming to support the comprehensive evaluation of cementing quality. By leveraging the interaction between X-Ray and the medium, the study applies regularized Newton's method to invert cement and formation parameters, enabling real-time evaluation of cement density. Through energy spectrum analysis with detectors at different spacing, key metrics such as cement density, cement thickness, formation density, and changes in volume photoelectric absorption cross-section index are analyzed. Through the analysis of energy spectrum, the forward model of different energy window



 ${\bf Fig.~9.}$ The response of the gamma flux to formation parameter.

Table 2The comparison between the actual values and the inversion values.

Model	Lithology	Cement thickness, cm	Inversion	Cement density, g⋅cm ⁻³	Inversion	Formation density, g·cm ⁻³	Inversion
M1	S	2.72	2.679	1.62	1.628	2.287	2.312
M2	S	3.19	3.087	1.92	1.929	2.37	2.308
M3	S	2.28	2.359	1.77	1.748	2.122	2.112
M4	L	1.62	1.856	1.83	1.825	2.402	2.364
M5	D	2.55	2.368	1.29	1.288	2.608	2.634
M6	S & L	2.09	1.951	1.68	1.681	2.294	2.274

Table 3 The parameters of each layer.

Layer	Formation med	ium	Cement				
	Volume fraction, %			Porosity, %	Density, g/cm ³	Thickness, cm	Density, g/cm ³
	Sandstone	Limestone	Dolomite				
A	51	22	27	12	2.516	3.31	1.54
В	39	16	45	29	2.249	2.52	1.62
C	27	44	29	9	2.584	2.25	2.17
D	37	16	47	17	2.463	3.35	1.25
Е	73	19	8	21	2.326	2.50	1.98
F	56	33	11	27	2.237	2.42	1.62
G	24	58	18	6	2.621	3.53	1.85

gamma counts on cement and formation parameters is established, and the interaction of multiple parameters is considered. By

utilizing the forward model, the regularized Newton's method enables rapid calculation of cement density and formation density

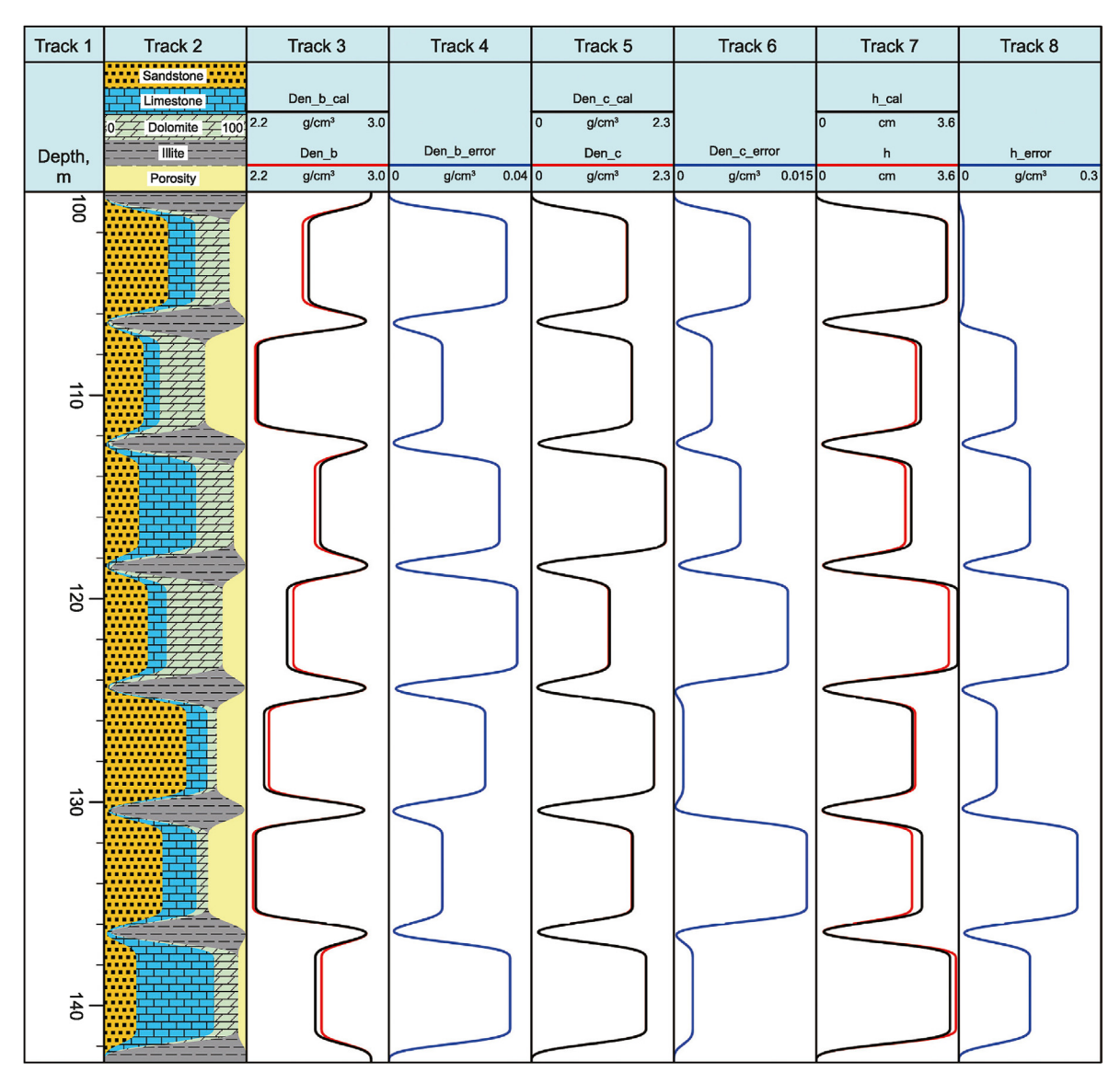


Fig. 10. The simulation example.

Table 4 The errors of each parameter.

Layer	Formation density, g/cm ³	Cement thickness, cm	Cement density, g/cm ³
Α	0.033	0.01	0.008
В	0.015	0.12	0.004
C	0.031	0.15	0.007
D	0.036	0.23	0.012
E	0.027	0.08	0.001
F	0.015	0.25	0.014
G	0.034	0.15	0.002

parameters. This approach maintains high accuracy, keeping the calculation error of cement density in cased well environment to within 0.015 g/cm³, comparable to the accuracy of open-hole density measurements. Additionally, the inversion results of formation density still guarantee the semi-quantitative calculation of

it. Future work will focus on further developing the calculation method for cement density under different casing sizes and casing damage environments to broaden the application of the proposed method.

CRediT authorship contribution statement

Ji-Lin Fan: Writing — original draft, Data curation. **Qiong Zhang:** Validation, Investigation, Conceptualization. **Ya Jin:** Data curation. **Quan-Wen Zhang:** Formal analysis.

Declaration of competing interest

The authors declared that they have no conflicts of interest to this work.

Acknowledgements

The authors would like to acknowledge the support of the National Natural Science Foundation of China (U23B20151 and 52171253) and National Science Foundation for Young Scientists of Sichuan (2025ZNSFSC1168).

References

- Baker, P.E., 1957. Density logging with gamma rays. Transactions of the AIME 210 (1), 289–294. https://doi.org/10.2118/940-G.
- Battistoni, G., Cerutti, F., Fasso, A., et al., 2007. The FLUKA code: description and benchmarking. AIP Conf. Proc. 896 (1), 31–49. https://doi.org/10.1063/1.2720455.
- Bayless, J.R., Burkhart, C.P., Kuthi, A., 1993. Advances in X-Ray and neutron source technologies for logging applications. SPWLA Annual Logging Symposium. SPWLA-1993-Y.
- Becker, A.J., Boyce, J.R., Corris, G.W., et al., 1987. Detection of scattered X-Ray from an electron linac in a borehole. Nucl. Instrum. Methods Phys. Res. Sect. B Beam Interact. Mater. Atoms 24, 995–998. https://doi.org/10.1016/s0168-583x(87) 80296-3.
- Bertozzi, W., Ellis, D.V., Wahl, J.S., 1981. The physical foundation of formation lithology logging with gamma rays. Geophysics 46 (10), 1439–1455. https:// doi.org/10.1190/1.1441151.
- Dowell, I.A., Seiler, D.D., York, P.L., 1999. Logging while drilling borehole imaging and dipmeter device. U.S. Patent 5, 899–958.
- Eyl, K.A., Chapellat, H., Chevalier, P., et al., 1994. High-resolution density logging using a three detector device. SPE Annual Technical Conference and Exhibition. SPE-28407-MS. https://doi.org/10.2118/28407-MS.
- Guo, W., Zannoni, S.A., Haramboure, C.E., et al., 2014. Method and system of determining a parameter associated with a formation corrected for neutrons produced. U.S. Patent. 8, 692, 185.

- Hu, Y., Guo, W., 2015. Behind-casing cement void volumetric evaluation. SPE Thermal Well Integrity and Design Symposium, SPE-178447-MS. https://doi.org/10.2118/178447-MS.
- Jussiani, E.I., Appoloni, C.R., 2015. Effective atomic number and density determination of rocks by X-Ray microtomography. Micron 70, 1–6. https://doi.org/10.1016/j.micron.2014.11.005.
- Li, O.Y., Wang, Y., Zhang, Q., et al., 2023. Parallel computing approach for efficient 3-D X-Ray-simulated image reconstruction. Nucl. Sci. Tech. 34 (7), 101. https://doi.org/10.1007/s41365-023-01264-6.
- Li, P., Lee, J., Coats, R., et al., 2019. New 4¼-in. ultrasonic LWD technology provides high-resolution caliper and imaging in oil-based and water-based muds. SPWLA Annual Logging Symposium. SPWLA-2019-T. https://doi.org/10.30632/T60ALS-2019 T.
- Li, Y., Zhang, Q., 2023. A novel constraint-based method for density measurement in cased hole. Geoenergy Science and Engineering 228, 211954. https://doi.org/10.1016/j.geoen.2023.211954.
- Moake, G.L., 1998. Design of a cased-hole-density logging tool using laboratory measurements. SPE Annual Technical Conference and Exhibition. SPE-49226-MS. https://doi.org/10.2118/49010-MS.
- Odom, R.C., Streeter, R.W., Wilson, R.D., 1999. Formation density measurement utilizing pulse neutrons. U.S. Patent 5, 900, 627. Reichel, N., Evans, M., Allioli, F., et al., 2012. Neutron-Gamma Density (NGD):
- Reichel, N., Evans, M., Allioli, F., et al., 2012. Neutron-Gamma Density (NGD): principles, field test results and log quality control of a radioisotope-free bulk density measurement. SPWLA Annual Logging Symposium. SPWLA-2012-082.
- Simon, M., Tkabladze, A., Beekman, S., et al., 2018. A revolutionary X-Ray tool for true sourceless density logging with superior performance. SPWLA Annual Logging Symposium. SPWLA-2018-G.
- Thierry, S., Klieber, C., Lemarenko, M., et al., 2016. New-generation ultrasonic measurements for quantitative cement evaluation in heavy muds and thickwall casings. SPE Annual Technical Conference and Exhibition. SPE-181450-MS. https://doi.org/10.2118/181450-MS.
- Wahl, J.S., Tittman, J., Johnstone, C.W., 1964. The dual spacing formation density log. J. Petrol. Technol. 16 (12), 1411–1416. https://doi.org/10.2118/989-PA.
- Wang, Y., Zhang, Q., 2023. A characterization study on perovskite X-Ray detector performance based on a digital radiography system. Nucl. Sci. Tech. 34 (5), 69. https://doi.org/10.1007/s41365-023-01220-4.
- Wilson, R.D., 1995. Bulk Density Logging with High-Energy Gammas Produced by Fast Neutron Reactions with Formation Oxygen Atoms. IEEE Nuclear Science Symposium and Medical Imaging Conference Record, pp. 209–213. https:// doi.org/10.1109/NSSMIC.1995.504211.
- Zhang, F., Fan, J., Liu, Y., et al., 2023. A new algorithm for evaluating reservoir density based on X-Ray logging technology. Appl. Radiat. Isot. 175, 109793. https://doi.org/10.1016/j.apradiso.2021.109793.
- Zhang, Q., Ge, Y., Li, Y.L., 2023. Source-less density measurement using an adaptive neutron-induced gamma correction method. Nucl. Sci. Tech. 34 (8), 125. https:// doi.org/10.1007/s41365-023-01274-4.
- Zhang, Q., Wang, Y., 2024. Formation density and photoelectric index calculation using an ultra-slim density tool. Geoenergy Science and Engineering 237, 212817. https://doi.org/10.1016/j.geoen.2024.212817.